A Direct Measurement of Charmed D Mesons Hardronic Decay Fractions at 4.03GeV

Kanglin He, Jimao Ma

P.O.Box 918-2, Beijing

June 1999

I. Introduction

The Absolute Beaching ratios for $D^0 \to K^-\pi^+$ and $D^+ \to K^-\pi^+\pi^+$ are very important for normalization of both D meson, B meson and Z^0 boson decay fraction. Most of D, B and Z^0 decay branching ratios are measured relative to $D^0 \to K^-\pi^+$ and $D^+ \to K^-\pi^+\pi^+$. The precisely measurement of the two branching ratios can directly improve the measurement the CKM matrix element. At present, many experiments, MarkI, MarkII, MarkIII, HRS, ALEPH, CLEO and ARGUS, have reported their measurements of $\mathrm{Br}(D^0 \to K^-\pi^+)$. MarkIII collaboration have determined the absolute branching ratio of $D^0 \to K^-\pi^+$ directly at $\psi(3770)$ with double-tags method. The high energy experiments selected decay chain $D^{*+} \to \pi^+ D^0, D^0 \to K^-\pi^+$ to measure the $\mathrm{Br}(D^0 \to K^-\pi^+)$. It was said that the measurement method of high energy experiment maybe had some model dependent factor. The results from MarKIII collaboration are little disagreement with the High-Energy e^+e^- collide experiments. But the MarKII measurement cannot explain the decay of B meson well.

Since 1992 to 1994, BES has collected the total amount of $22.3pb^{-1}$ data at $\sqrt{s}$ = 4.03GeV. Based on this data sample, we could find about 8000 D^0 tags and 2700 D^+ tags. The $\sqrt{s}$ = 4.03GeV is just greater than the threshold of $D^*\overline{D^*}$ production. Charmed D meson may come from the $D\overline{D}$, $D\overline{D^*}$ and $D^*\overline{D^*}$ production procedures, including charged and neutral channel. The decay of $D^{*+} \to \pi^+ D^0$ raised the mixing of D^0 and D^+ in final state. The soft γ and $\pi^{0\pm}$ from D^* meson decay are difficult to be reconstructed by BES detector, and the method of beam-energy-constraint and kinematic fitting technique are not avaiable. However, the total number of D meson tags we got are as 2.5 times large as that of MarKIII. The large data sample would make it possible to obtain the absolute hadronic decay branching ratio of charmed D mesons at the precision level of MarKIII measurement.

II. The Method of Combining Single-tags and Double-tags

To measure the absolute branching ratio of D mesons, a new technique was developed which doesn't rely on the decay fractions of D^* meson and the determination of charmed D

meson production cross sections. At $\sqrt{s} = 4.03$GeV energy region, we assumed that events containing charmed D mesons arise from $D\overline{D^*}$ and $D^*\overline{D^*}$ productions (the $D\overline{D}$ procedure were ignored because of the small production cross section and a momentum cut which will be illustrated later), so that the detection of a single D in an event implies that the recoiling system is a monochromatic $\overline{D}$ or a $\overline{D}$ decay from D^* mesons. For the D^0 tag, it may comes from neutral charmed D pair productions or charged charmed D pair productions. For the D^+ tag, it comes solely from the charged charmed D pair productions. We assumed that the neutral D^* mesons total decay to D^0 mesons with a 100% decay fractions because of the kinematics limitation, the charged D^* mesons are decayed to D^0 meson with a decay fractions $\mathrm{Br}(D^{*+} \to \pi^+ D^0)$ and D^+ mesons with a decay fractions $1 - \mathrm{Br(D^{*+} \to \pi^+ D^0)}$. Table.1 listed the observed possibility of single-tags and double-tags via different charmed D mesons productions.

The data are searched for events containing either one or two reconstructed D mesons. For this analysis, two D^0 decay channels($K^-\pi^+$, $K^-\pi^+\pi^+\pi^-$) and one D^+ decay channel ($K^-\pi^+\pi^+$) are considered. The momentum distributions of reconstructed D tags provided an additional information to identify the $D\overline{D}$,$D\overline{D^*}$,$D^*\overline{D^*}$ productions (see Figure.1). By comparing the observed number of a single D is reconstructed with the number of partial reconstructed $D\overline{D}$ events for different charmed D meson productions, we could employed a χ^2 minimization fit. The individual D meson branching ratio could be derived independently of σ_D.

The momentum distributions are monochromatic for $D\overline{D}$ production and the directly D meson rise from $D\overline{D^*}$ procedure. It's different for D meson decay from D^* meson. The momentum distribution of tagged D approximates monochromatic while D^* meson decaying to $\pi^0 D$ or $\pi^+ D^0$ due to the low decay Q value, but it becomes very wide while D^* decaying to γD. The total momentum spectrum consists of the distribution of D tags from different productions and from the different decay modes of D^* mesons, combined with the background.The individual distributions of tagged D momentum are overlapped, especially for the D meson arise from the decay $D^* \to \gamma D$, which is hard to be distinguished from the background distribution. In order to reduce the system uncertainty, the momentum cut should make the detection efficiency to be united for the decay $D^* \to \gamma(\pi^0)D$ and eliminate the overlap of $D\overline{D}$, $D\overline{D^*}$, $D^*\overline{D^*}$ productions procedure. The Monte Carlo study show that the momentum cut listed in Table.2 will raise a small system uncertainty of detector acceptance caused by the decay $D^* \to \gamma(\pi^0)D$ as following:

$$\frac{\Delta\epsilon}{\epsilon} = \begin{cases} < 2\% & \text{(for single-tag events)} \\ < 4\% & \text{(for double-tag events)} \end{cases} \tag{1}$$

It implied that we could use the $D\overline{D^*}$ and $D^*\overline{D^*}$ generator in BESLIB directly to evaluate the acceptance of single-tags and double-tags.

III. Single-tag Selection

Single-tag candidates selection proceeds as follows. The charged particles are required to satisfy $|\cos\theta| < 0.85$(where θ is the polar angle with respect to the beam) to insure a reliable measurement by MDC. The the preliminary vertex of a charged particle is required to lie within $|V_{xy}| < 1.2$cm and $|V_z| < 15$cm to suppress the background from beam gas and cosmic rays. A charged particle is assigned to π or K by requiring a likelihood greater than 1%, according to TOF and dE/dx information. Additionally, Kaon hypothesis should have a relative likelihood greater than that of Pion's. Appropriate combinations of charged tracks are formed for the two D^0 and one D^+ decay modes under study.

In the case of the $D\overline{D}$ production, the energy of each D candidate is constrained to the beam energy($|E - E_b|$ <50MeV) to improve mass resolution and further reduce background. Events passed the above criteria are fit to the hypothesis:

$$e^+e^- \rightarrow \psi(4030) \rightarrow K(\mathrm{n})\pi + \mathrm{X(missing)}$$

where $M_X = M_{Kn\pi}$. The fits with $\chi^2 > 15$ are removed. Figure 2 show the invariant mass distributions of decay $D^0 \rightarrow K^-\pi^+$ and $D^+ \rightarrow K^-\pi^+\pi^+$.The mass plot are fitted with a Gaussian for the signal and a linear polyominal for the background. There are 134 ± 27 events for $D^0 \rightarrow K^-\pi^+$ and 164 ± 34 events for $D^+ \rightarrow K^-\pi^+\pi^+$ above background. No clearly D signal was found for the decay of $D^0 \rightarrow K^-\pi^+\pi^+\pi^-$. The number of events obtained from the $D\overline{D}$ production is so little that it will be discarded for further analysis. To separate the $D\overline{D^*}$ and $D^*\overline{D^*}$ charmed D meson production mode and further reduce background, the momentum cut listed in Table 2 is applied to each D candidate. The resulting mass distributions for the single-tag modes are shown in Figure 3. In each case, the invariant mass plot are fitted using a Gaussian above a 2^{th} polynomial background.

The number of events need to be modified by a double counting correction. The double counting was raised by particle misidentification, wrong combination and rare double-tag events. To evaluate the double counting distribution, we scan the whole mass plot from the center of M_D peak with the size of $2 \times 3\sigma$ mass region by a step 0.25σ to the left and right side. Figure 4 show the double counting distribution for each single-tag. In figure 4, it was fitted using a Gaussian for signal region($|M - M_D| < 3\sigma_M$) and a 3^{rd} order polynomial for background region. The fit provided the number of double counted events for each scanned mass region. The pure number of events(N_{pure}) in signal region is defined as

$$N_{\mathrm{pure}} = N_{\mathrm{total}} - N_{DC}^{sg} \quad , \quad N_{DC}^{sg} = N_{DC}^{\mathrm{total}} - N_{DC}^{bg} \tag{2}$$

the double counting ratio is defined as

$$R_{DC} = \frac{N_{DC}^{sg}}{N_{\mathrm{total}}} \times 100\% \tag{3}$$

where N_{total} is the number of signal events, N_{DC}^{total} is the total number of double counted events in signal region which is calculated by simply counting, N_{DC}^{bg} is the number of double counted background events in signal region which was obtained from fit, N_{DC}^{sg} is the number of double counted signal events. To compute the statistic error after double counting, $\sigma_{N_{DC}^{sg}}$ is taken as $\sqrt{N_{DC}^{sg}}$. This will lead to :

$$\sigma_{N_{\mathrm{pure}}} = \sqrt{\sigma_{N_{\mathrm{total}}}^2 + N_{DC}^{sg}} \tag{4}$$

IV. Double-Tag Selection

Double-tags are subject to additional constraints. Events are partial reconstructed to the hypothesis:

$$\begin{aligned} e^+e^- &\to \psi(4030) \\ &\to \left\{D\overline{D^*}, D^*\overline{D^*}\right\} \\ &\to \underbrace{D\overline{D}}_{\text{reconstructed}} + \underbrace{X \to \gamma, \pi^{0,\pm}}_{\text{missing}} \end{aligned} \tag{5}$$

where the possible $D\overline{D}$ pairs are one of the following combinations:

$$\left.\begin{array}{rcl} D^0 \to K^-\pi^+ & \text{vs} & \overline{D^0} \to K^+\pi^- \\ D^0 \to K^-\pi^+ & \text{vs} & \overline{D^0} \to K^+\pi^-\pi^-\pi^+ \\ D^0 \to K^-\pi^+\pi^+\pi^- & \text{vs} & \overline{D^0} \to K^+\pi^-\pi^-\pi^+ \\ D^0 \to K^-\pi^+ & \text{vs} & D^- \to K^+\pi^-\pi^- \\ D^0 \to K^-\pi^+\pi^+\pi^- & \text{vs} & D^- \to K^+\pi^-\pi^- \\ D^- \to K^-\pi^+\pi^+ & \text{vs} & D^- \to K^+\pi^-\pi^- \end{array}\right\} \text{ and } \begin{array}{c}\text{charge}\\ \text{conjugation}\end{array} \tag{6}$$

Figure 5 show the invariant mass distribution of recoiling system while the mass in tag-side satisfies $|M_{\text{tag}} - M_D| < 3\sigma_M$. In each case, the mass plot is fitted with a Gaussian and a linear background. The results are summarized in table 3. Since the number of double tag events obtained from tag-side is not as the same as that obtained from recoil side, we take the average number out of tag side and recoil side.

V. Measurement of Br$(D^0 \to K^-\pi^+)$, Br$(D^0 \to K^-\pi^+\pi^+\pi^-)$, Br$(D^+ \to K^-\pi^+\pi^+)$ and Br$(D^{*+} \to \pi^+D^0)$

To determine the individual branching ratios(B_i) and the number of produced $D\overline{D^*}$, $D^*\overline{D^*}$ pairs ($N = \sigma L$), the observed number of single-tags(S_i) and double-tags(D_{ij}) can be expected as (see table 1):

$$\left.\begin{array}{rcl} S_i^0 &=& 2N^0\epsilon_i B_i + N^+\epsilon_i B_i B_+^0 \\ S_i^+ &=& N^+\epsilon_i B_i + N^+\epsilon_i B_i(1 - B_+^0) \\ D_{ij}^{00} &=& \delta_{ij} N^0 \epsilon_{ij} B_i B_j \\ D_{ij}^{++} &=& \delta_{ij} N^+ \epsilon_{ij} B_i B_j (1 - B_+^0) \\ D_{ij}^{0+} &=& N^+\epsilon_{ij} B_i B_j B_+^0 \end{array}\right\} \text{ for } \mathrm{D\overline{D^*}} \text{ production} \tag{7}$$

and

$$\left.\begin{array}{rcl} S_i^0 &=& 2N^0\epsilon_i B_i + 2N^+\epsilon_i B_i B_+^0 \\ S_i^+ &=& 2N^+\epsilon_i B_i(1 - B_+^0) \\ D_{ij}^{00} &=& \delta_{ij}(N^0 \epsilon_{ij} B_i B_j + N^+\epsilon_{ij} B_i B_j (B_0^+)^2) \\ D_{ij}^{++} &=& \delta_{ij} N^+ \epsilon_{ij} B_i B_j (1 - B_+^0)^2 \\ D_{ij}^{0+} &=& 2N^+\epsilon_{ij} B_i B_j B_+^0 (1 - B_+^0) \end{array}\right\} \text{ for } \mathrm{D^*\overline{D^*}} \text{ production} \tag{8}$$

with $N^0 = \sigma_{D^0\overline{D^{*0}}} \times L$ and $N^+ = \sigma_{D^\pm D^{*\mp}} \times L$ in equation(7), $N^0 = \sigma_{D^{*0}\overline{D^{*0}}} \times L$ and $N^+ = \sigma_{D^{*\pm}D^{*\mp}} \times L$ in equation(8), and where $B_{i,j}$ is the individual branching fractions in $\{i,j\}^{\text{th}}$ D decay mode, ϵ_i is the efficiency for reconstructing a single-tag in the i^{th} D decay mode, ϵ_{ij} is the partial reconstruction efficiency for $D\overline{D}$(from $D\overline{D^*}$ and $D^*\overline{D^*}$) decay mode i and j, $B_+^0 = \mathrm{Br}(\mathrm{D}^{*+} \to \pi^+\mathrm{D}^0)$. The efficiencies are determined by a detail Monte Carlo simulation of $D\overline{D^*}$, $D^*\overline{D^*}$ production and decay, including the detector response. In final, we form a χ^2 expression:

$$\chi^2 = \sum_i \frac{(S^i_{\text{measure}} - S^i_{\text{predict}})^2}{\sigma^2_{S^i_{\text{measure}}}} + \sum_{ij} \frac{(D^{ij}_{\text{measure}} - D^{ij}_{\text{predict}})^2}{\sigma^2_{D^{ij}_{\text{measure}}}} \tag{9}$$

where, the index {measure,predict} represent for the number of tags obtained from {measurement, prediction}, σ are the errors of measurement.

A χ^2 minimization fit was employed by over all tags (S for single-tags, D for double-tags) and over all production modes($D\overline{D^*}$ and $D^*\overline{D^*}$, including charged and neutral channel), yielding $(5.48 \pm 1.14) \times 10^4$ produced $D^0\overline{D^{*0}}$ events and c.c, $(5.16 \pm 1.46) \times 10^4$ produced $D^{*\pm}D^\mp$ events, $(4.61 \pm 0.83) \times 10^4$ produced $D^{*0}\overline{D^{*0}}$ events and $(1.94 \pm 0.50) \times 10^4$ produced $D^{*\pm}D^{*\mp}$ events(where the error is statistic). A comparison of the observed numbers of tags with the prediction from the fit is shown in table 4(for $D\overline{D^*}$ production) and table 5(for $D^*\overline{D^*}$ production). The fit yields a χ^2 of 4.95 for 10 degrees of freedom. The fitted values for D decay branching fractions and the branching ratio of $D^{*+} \to \pi^+ D^0$ are obtained:

$$\begin{array}{rcl} \mathrm{Br}(\mathrm{D}^0 \to \mathrm{K}^-\pi^+) & = & (3.95 \pm 0.58 \pm 0.26)\% \\ \mathrm{Br}(\mathrm{D}^0 \to \mathrm{K}^-\pi^+\pi^+\pi^-) & = & (8.24 \pm 1.12 \pm 0.57)\% \\ \mathrm{Br}(\mathrm{D}^+ \to \mathrm{K}^-\pi^+\pi^+) & = & (9.6 \pm 2.9 \pm 1.4)\% \\ \mathrm{Br}(\mathrm{D}^{*+} \to \pi^+\mathrm{D}^0) & = & (51 \pm 11 \pm 5)\% \end{array} \tag{10}$$

where the first error is statistical and the second is systematic.

The systematic errors on the fitted branching ratios arise from several sources. The uncertainty in charged particle tracking efficiency and particle identification contributes $2 \sim 10\%$ in final measurement. The determination of the number of double-tags raised less than 4% uncertainty. The uncertainty in the decay fractions of $D^* \to \gamma(\pi^0)D$ is less than 4% which has been illustrated in section II. The uncertainty in detector simulation is estimated about 5%. The systematic errors from the different sources are summarized in table 6.

VI. Measurement of Br$(D^0 \to \overline{K^0}\pi^+\pi^-)$

The branching ratio of $D^0 \to \overline{K^0}\pi^+\pi^-$ is an important constant to normalize the branching fractions of D^0 decay to the final state which contains one K^0 meson. In this section, the measurement of the absolute branching ratio $D^0 \to \overline{K^0}\pi^+\pi^-$ is presented.

The event selection proceeds the same criteria described in section III excepts the vertex cut for tracks from K^0 decay. Neutral Kaons are detected through the decay $K^0_S \to \pi^+\pi^-$, where the $\pi^+\pi^-$ invariant mass is required to lie within 20MeV/c^2 of the K^0_S mass. The $\pi^+\pi^-$ secondary vertex is required to be more than 4mm apart away from the beam axis, and the position vector of the vertex and the momentum vector of K^0_S is required to align in xy-plane (An open angle cut θ with $\cos\theta$ is applied). The mass distribution and the double counting distribution of $K_S^0\pi^+\pi^-$ are shown in figure 6. Since the charm quantum number is not determined by K_S^0, we only use the single-tag in measurement. The expected number of single-tags for decay $D^0 \to \overline{K^0}\pi^+\pi^-$ can be expressed as:

$$\begin{array}{rcll} S & = & 2N^0\epsilon B + N^+\epsilon BB_+^0 & \text{for } D\overline{D^*} \text{ production} \\ S & = & 2N^0\epsilon B + 2N^+\epsilon BB_+^0 & \text{for } D^*\overline{D^*} \text{ production} \end{array} \tag{11}$$

An additional

$$\chi^2_{\rm add} = \sum_i \frac{(S^i_{\rm measure} - S^i_{\rm predict})^2}{\sigma^2_{S^i_{\rm measure}}} \quad (i = D\overline{D^*}, D^*\overline{D^*}) \tag{12}$$

is formed and added to equation (9). The χ^2 fit yields

$$\mathrm{Br}(\mathrm{D}^0 \to \overline{\mathrm{K}^0}\pi^+\pi^-) = (5.46 \pm 0.95 \pm 0.40)\% \tag{13}$$

The observed number of tags (445 ± 80 for $D\overline{D^*}$, 421 ± 44 for $D^*\overline{D^*}$) agrees well with the prediction from the fit (468 for $D\overline{D^*}$, 413 for $D^*\overline{D^*}$).

The systematic error are estimated by varying the event selection criteria, the uncertainty in Monte Carlo simulation and generation. The event selection for $D^0 \to K^-\pi^+$, $D^0 \to K^-\pi^+\pi^+\pi^-$ and $D^+ \to K^-\pi^+\pi^+$ contributes 4.5% to the uncertainty in final measurement. The uncertainty on $D^0 \to K_S^0\pi^+\pi^-$ event selection is estimated to be 2.5%. The Monte Carlo simulation raise a 5% uncertainty, and the systematic uncertainty arise from the momentum cut is less than 2%.

VII. Discussion and Conclusion

Figure 7 show the comparison of our measurements with the results from other experiments. The measurements of $\mathrm{Br}(D^0 \to K^-\pi^+)$ is consistent with the results in recent years from the ALEPH, CLEO and AUGUS experiments. The results of $\mathrm{Br}(D^0 \to K^-\pi^+\pi^+\pi^-)$ and $\mathrm{Br}(D^0 \to \overline{K^0}\pi^+\pi^-)$ would be helpful to improve the precision of the world average values. The errors of two branching ratios, $\mathrm{Br}(D^+ \to K^-\pi^+\pi^+)$ and $\mathrm{Br}(D^{*+} \to \pi^+D^0)$, are significantly large due to the limitation of D^+ sample and the mixing of D^0 and D^+ in final states. The value of $\mathrm{Br}(D^{*+} \to \pi^+D^0)$ favors the results from the MarkI, MarkII and MarkIII experiments. It's agreement with the previous measurement of BES:

$$\begin{array}{ll} \mathrm{Br}(\mathrm{D}^{*+} \to \pi^+\mathrm{D}^0) = (68.8^{+10.2+5.3}_{-24.2-5.5})\% & \text{(Double-tags method)} \\ \mathrm{Br}(\mathrm{D}^{*+} \to \pi^+\mathrm{D}^0) = (66.7 \pm 5.9 \pm 10.8)\% & \text{(Single-tags method)} \end{array} \tag{14}$$

but lower than the world average value $\mathrm{Br}(\mathrm{D}^{*+} \to \pi^+\mathrm{D}^0) = (68.3 \pm 1.4)\%$.

It is noticed that our measurements of $\mathrm{Br}(D^0 \to K^-\pi^+)$, $\mathrm{Br}(D^0 \to K^-\pi^+\pi^+\pi^-)$ and $\mathrm{Br}(D^+ \to K^-\pi^+\pi^+)$ fit the world average value very well. To lower the statistic errors of the observed charmed D meson production cross sections at $\sqrt{s} = 4.03$GeV, we take the world average value:

$$\begin{array}{rcl} \mathrm{Br}(\mathrm{D}^0 \to \mathrm{K}^-\pi^+) & = & (3.88 \pm 0.09)\% \\ \mathrm{Br}(\mathrm{D}^0 \to \mathrm{K}^-\pi^+\pi^+\pi^-) & = & (7.5 \pm 0.6)\% \\ \mathrm{Br}(\mathrm{D}^+ \to \mathrm{K}^-\pi^+\pi^+) & = & (9.1 \pm 0.7)\% \end{array} \tag{15}$$

Modes		Single Tags		Double Tags		
		D^0	D^+	D^0 as $\overline{D^0}$	D^+ vs D^-	D^0 vs D^-
$D\overline{D^*}$	0	$2\epsilon_i B_i$	0	$\delta_{ij}\epsilon_{ij}B_iB_j$	0	0
	$\pm$	$\epsilon_i B_i B_0^+$	$\epsilon_i B_i(1+B_+^+)$	0	$\delta_{ij}\epsilon_{ij}B_iB_jB_+^+$	$\epsilon_{ij}B_iB_jB_0^+$
$D^*\overline{D^*}$	0	$2\epsilon_i B_i$	0	$\delta_{ij}\epsilon_{ij}B_iB_j$	0	0
	$\pm$	$2\epsilon_i B_i B_0^+$	$2\epsilon_i B_i B_+^+$	$\delta_{ij}\epsilon_{ij}B_iB_j(B_0^+)^2$	$\delta_{ij}\epsilon_{ij}B_iB_j(B_+^+)^2$	$2\epsilon_{ij}B_iB_jB_0^+B_+^+$
$D\overline{D}$	0	$2\epsilon_i B_i$	0	$\delta_{ij}\epsilon_{ij}B_iB_j$	0	0
	$\pm$	0	$2\epsilon_i B_i$	0	$\delta_{ij}\epsilon_{ij}B_iB_j$	0

Table 1: The observation possibility of single-tags and double-tags at $\sqrt{s}$=4.03GeV. Here, B_i, B_j are the decay fraction of $D \to (i^{th}, j^{th})$ tagged channels, ϵ_i is the acceptance of single-tags, ϵ_{ij} is the acceptance of double-tags, B_+^0 =Br($D^{*+} \to \pi^+ D^0$), $B_+^+ = 1 - B_+^0$, the symbol $\delta_{ij} = \begin{cases} 1(i=j) \\ 2(i \neq j) \end{cases}$. The acceptance ϵ was weighted by detection efficiencies for D meson arise from different decay mode of D^* mesons.

	$D\overline{D^*}$(unit:GeV/c)	$D^*\overline{D^*}$(unit:GeV/c)
D^0 Tag	0.36< p_D <0.70	0.02< p_D <0.32
D^+ Tag	0.36< p_D <0.70	0.02< p_D <0.30

Table 2: Momentum cut for single D tags selection.

as the inputs in equation (9). From the χ^2 minimization fit, we obtained

$$\begin{aligned} \sigma(D^0\overline{D^{*0}}) &= (2.57 \pm 0.18 \pm 0.20)\text{nb} \\ \sigma(D^{\pm}D^{*\mp}) &= (2.42 \pm 0.18 \pm 0.24)\text{nb} \\ \sigma(D^{*0}\overline{D^{*0}}) &= (2.19 \pm 0.16 \pm 0.18)\text{nb} \\ \sigma(D^{*\pm}D^{*\mp}) &= (0.89 \pm 0.16 \pm 0.07)\text{nb} \\ \mathrm{Br(D^{*+} \to \pi^+ D^0)} &= (50 \pm 8 \pm 4)\% \end{aligned} \tag{16}$$

where, the second error is systematic which including the contribution from different sources(see table 7 for detail). The ratios of, $D^0\overline{D^{*0}}$ to $D^{*0}\overline{D^{*0}}$, $D^{\pm}D^{*\mp}$ to $D^{*\pm}D^{*\mp}$ and $D^0\overline{D^{*0}}$ to $D^{*\pm}D^{\mp}$, are not constrained in the fit, but the measured results agree well with the ratios(quoted in equation(17)) predicted by the coupled channel model.

$$\begin{aligned} \sigma(D^0\overline{D^{*0}}) : \sigma(D^{*0}\overline{D^{*0}}) &= 1.17 \pm 0.18 \quad (1.35) \\ \sigma(D^{\pm}D^{*\mp}) : \sigma(D^{*\pm}D^{*\mp}) &= 2.72 \pm 0.62 \quad (2.69) \\ \sigma(D^0\overline{D^{*0}}) : \sigma(D^{\pm}D^{*\mp}) &= 1.06 \pm 0.17 \quad (1.08) \end{aligned} \tag{17}$$

Mode	Double-tag channel	Tag side	Recoil side	Average
$D\overline{D^*}$	$K^-\pi^+$ vs $K^+\pi^-$	18.2 ± 5.6	18.3 ± 6.8	18 ± 7
	$K^-\pi^+$ vs $K^+\pi^-\pi^-\pi^+$	33.9 ± 7.3	34.5 ± 7.1	34 ± 7
	$K^-\pi^+\pi^+\pi^-$ vs $K^+\pi^-\pi^-\pi^+$	20.3 ± 6.0	17.2 ± 5.9	19 ± 6
	$K^-\pi^+$ vs $K^+\pi^-\pi^-$	13.8 ± 5.2	15.5 ± 4.4	15 ± 5
	$K^-\pi^+\pi^+\pi^-$ vs $K^+\pi^-\pi^-$	15.5 ± 5.5	21.4 ± 5.1	18 ± 7
	$K^-\pi^+\pi^+$ vs $K^+\pi^-\pi^-$	25.2 ± 6.2	25.3 ± 5.9	25 ± 6
$D^*\overline{D^*}$	$K^-\pi^+$ vs $K^+\pi^-$	27.2 ± 5.8	23.0 ± 5.9	25 ± 6
	$K^-\pi^+$ vs $K^+\pi^-\pi^-\pi^+$	34.8 ± 6.8	42.7 ± 7.1	39 ± 8
	$K^-\pi^+\pi^+\pi^-$ vs $K^+\pi^-\pi^-\pi^+$	12.4 ± 4.6	13.2 ± 4.2	13 ± 5
	$K^-\pi^+$ vs $K^+\pi^-\pi^-$	5 ± 3		5 ± 3
	$K^-\pi^+\pi^+\pi^-$ vs $K^+\pi^-\pi^-$	5 ± 3		5 ± 3
	$K^-\pi^+\pi^+$ vs $K^+\pi^-\pi^-$	5 ± 3		5 ± 3

Table 3: The number of double-tag events.

Double-tags	$K^-\pi^+$	$K^-\pi^+\pi^+\pi^-$	$K^-\pi^+\pi^+$
$K^+\pi^-$ (fit)	18 ± 7 17	34 ± 7 36	15 ± 5 15
$K^+\pi^-\pi^-\pi^+$ (fit)		19 ± 6 20	18 ± 7 16
$K^+\pi^-\pi^-$ (fit)			25 ± 5 25
Single-tags (fit)	2294 ± 122 2326	1847 ± 165 1741	2207 ± 130 2218

Table 4: Comparison of single and double-tag measurements and fit results for $D\overline{D^*}$ production

Double-tags	$K^-\pi^+$	$K^-\pi^+\pi^+\pi^-$	$K^-\pi^+\pi^+$
$K^+\pi^-$ (fit)	25 ± 6 17	39 ± 8 33	5 ± 3 6
$K^+\pi^-\pi^-\pi^+$ (fit)		13 ± 5 19	5 ± 3 6
$K^+\pi^-\pi^-$ (fit)			5 ± 3 5
Single-tags (fit)	1981 ± 78 1994	1781 ± 90 1770	636 ± 80 619

Table 5: Comparison of single and double-tag measurements and fit results for $D^*\overline{D^*}$ production

Systematic Errors	Events selection		Detection Efficiency		Total
	Particle identification	Determination of Double-tags	Monte Carlo Simulation	Momentum CUT	
$\mathrm{Br}(D^0 \to K^-\pi^+)$	0.06	0.13	0.20	0.16	0.26
$\mathrm{Br}(D^0 \to K^-\pi^+\pi^+\pi^-)$	0.13	0.26	0.41	0.33	0.57
$\mathrm{Br}(D^+ \to K^-\pi^+\pi^+)$	1.2	0.40	0.48	0.39	1.4
$\mathrm{Br}(D^{*+} \to \pi^+ D^0)$	3.5	1.2	2.5	2.1	5.0

Table 6: Systematic errors on branching ratio fit (%).

Error Sources	$\sigma(D^0\overline{D^{*0}})$	$\sigma(D^\pm D^{*\mp})$	$\sigma(D^{*0}\overline{D^{*0}})$	$\sigma(D^{*\pm}D^{*\mp})$
Quotation of Branching Ratio	0.09	0.17	0.09	0.04
Monte Carlo Simulation	0.13	0.12	0.11	0.04
Momentum CUT	0.10	0.10	0.09	0.04
Luminosity Measurement	0.06	0.06	0.05	0.02
Total	0.20	0.24	0.18	0.07

Table 7: Systematic errors for cross section measurement (nb).

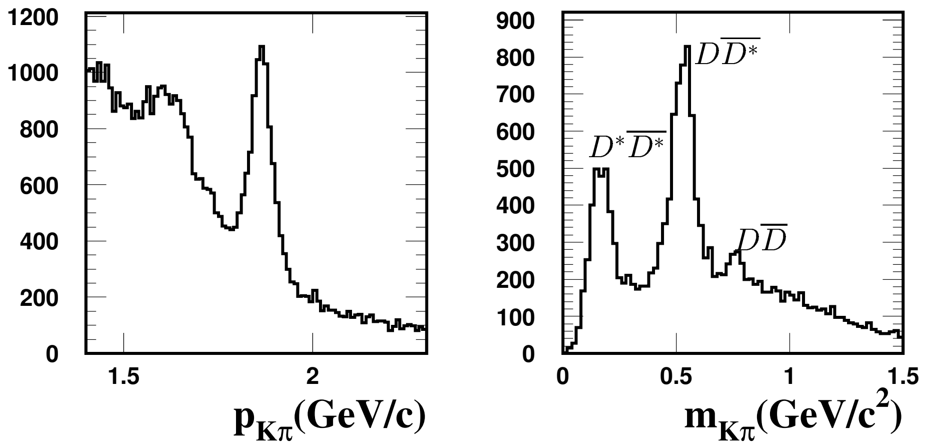

Figure 1: Momemtum and invariant mass distribution for tag $D^0 \to K^-\pi^+$.

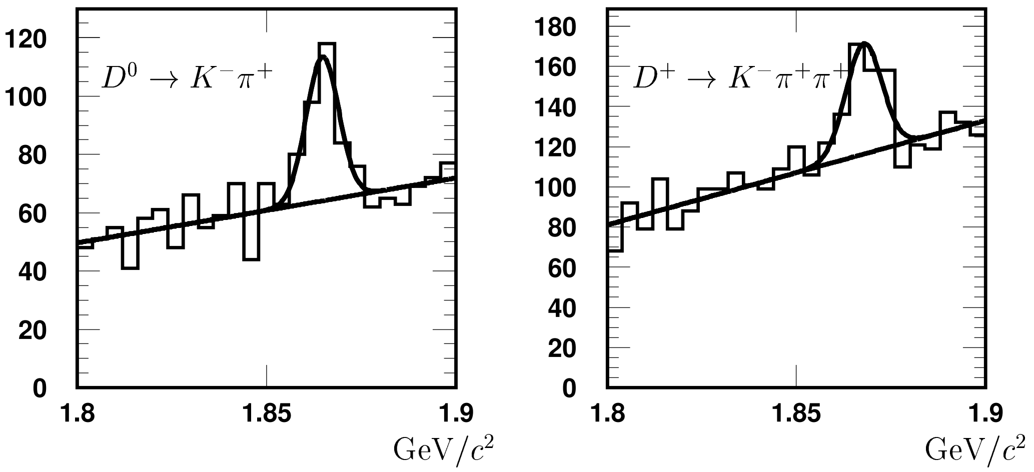

Figure 2: $M_{K\pi}$ and $M_{K\pi\pi}$ distribution in $D\overline{D}$ production.

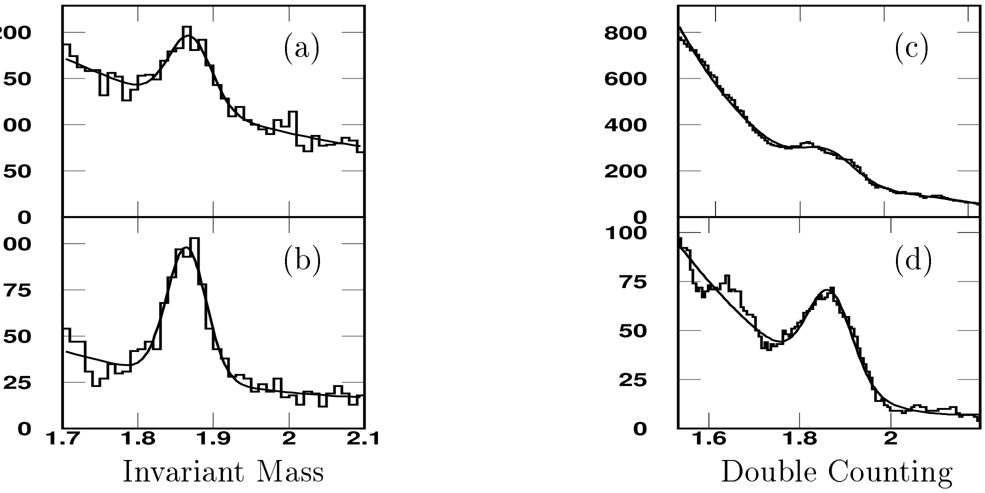

Figure 3: Invariant mass and double counting distributions for the decay $D^0 \to \overline{K^0}\pi^+\pi^-$. Where, (a) and (c) show the distribution for $D\overline{D^*}$ production, (c) and (d) show the distribution for $D^*\overline{D^*}$ production.

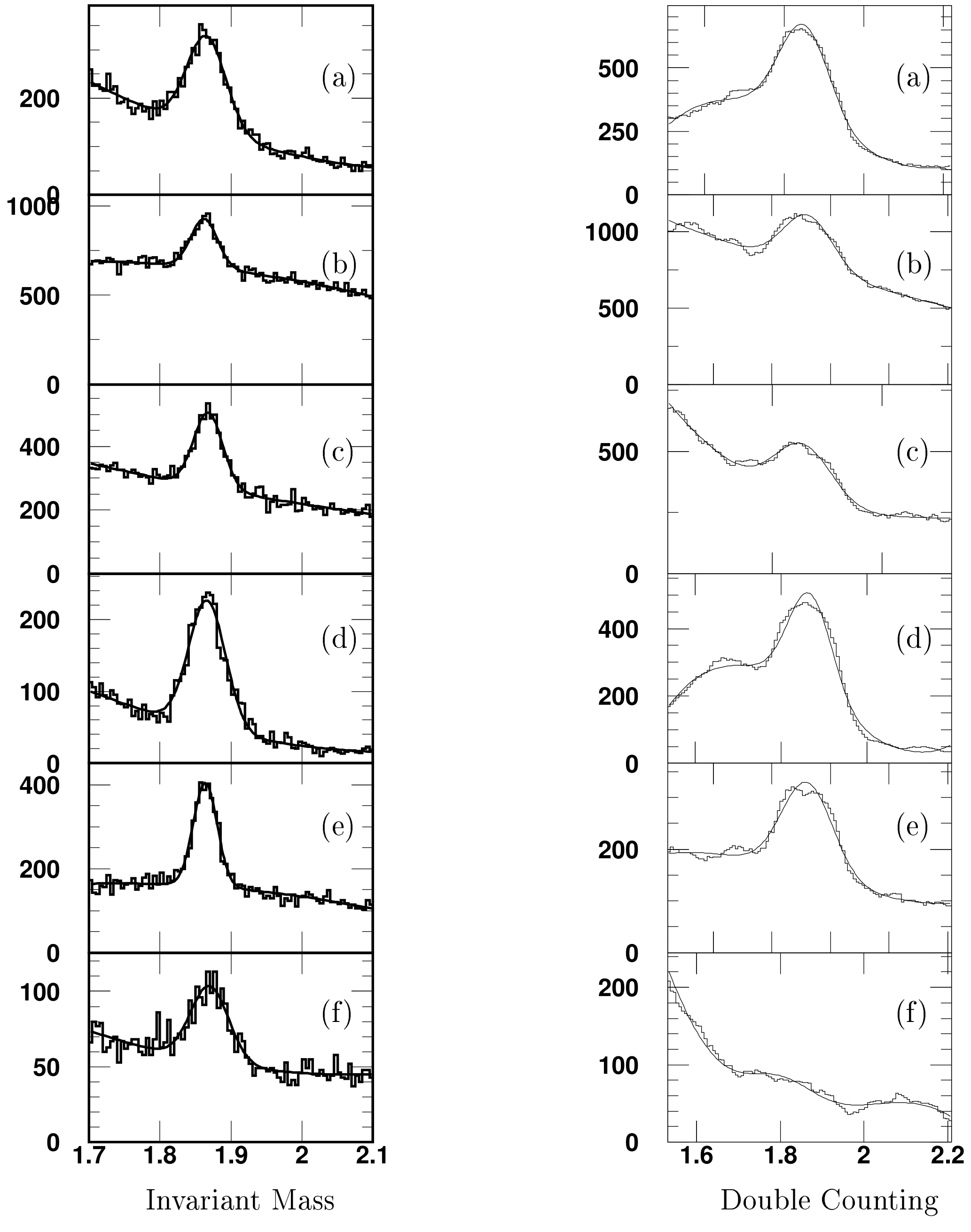

(a),(d):$D^0 \to K^-\pi^+$. (b),(e):$D^0 \to K^-\pi^+\pi^+\pi^-$. (c),(f):$D^+ \to K^-\pi^+\pi^+$

(a),(b),(c) for $D\overline{D^*}$, (e),(f),(g) for $D^*\overline{D^*}$

Figure 4: Invariant mass and double counting distributions for $D^0 \to K^-\pi^+$, $D^0 \to K^-\pi^+\pi^+\pi^-$ and $D^+ \to K^-\pi^+\pi^+$.

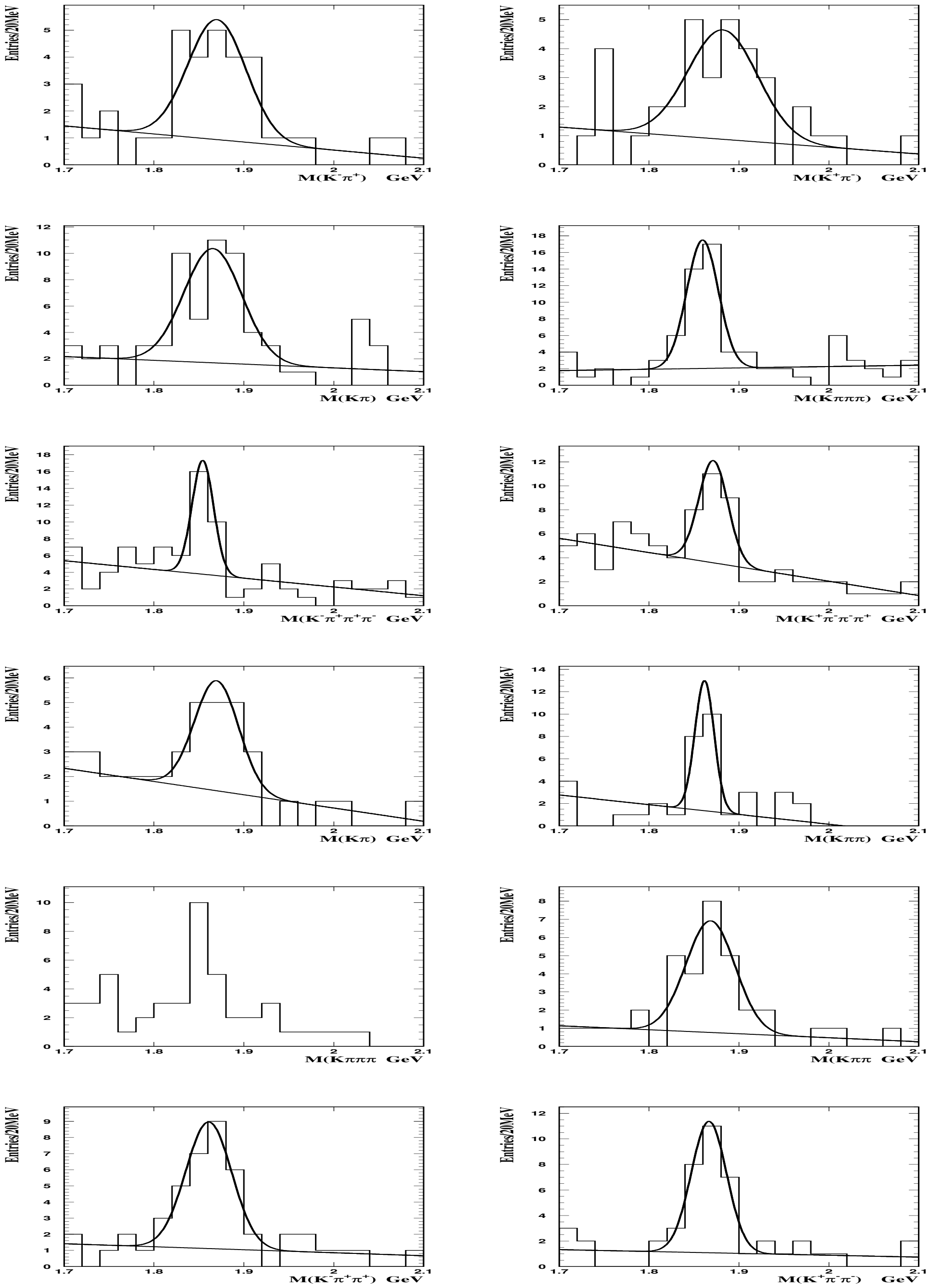

Figure 5: Invariant mass distribution of double-tag events(for $D\overline{D^*}$ production).

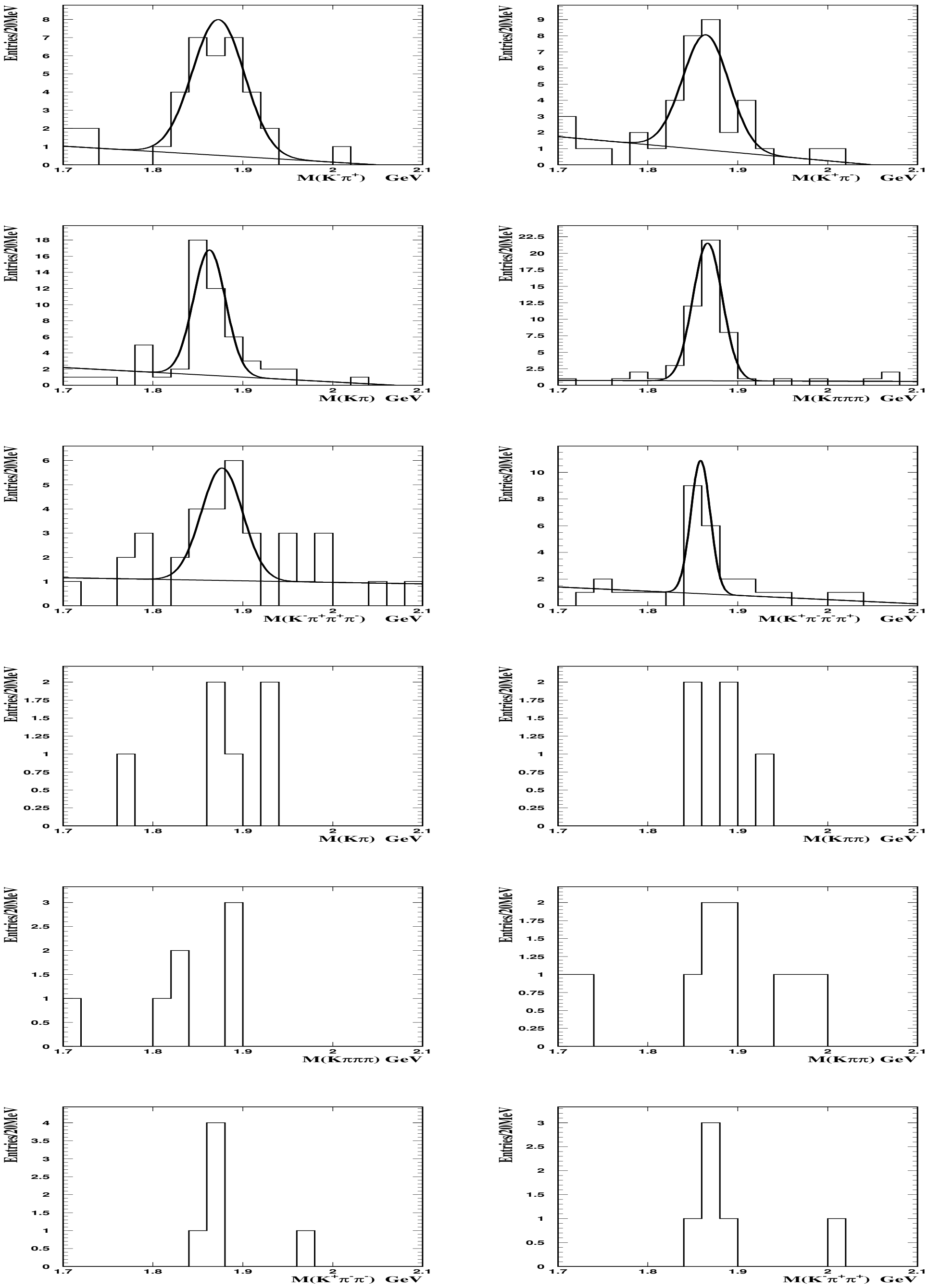

Figure 6: Invariant mass distribution of double-tag events(for $D^*\overline{D^*}$ production).

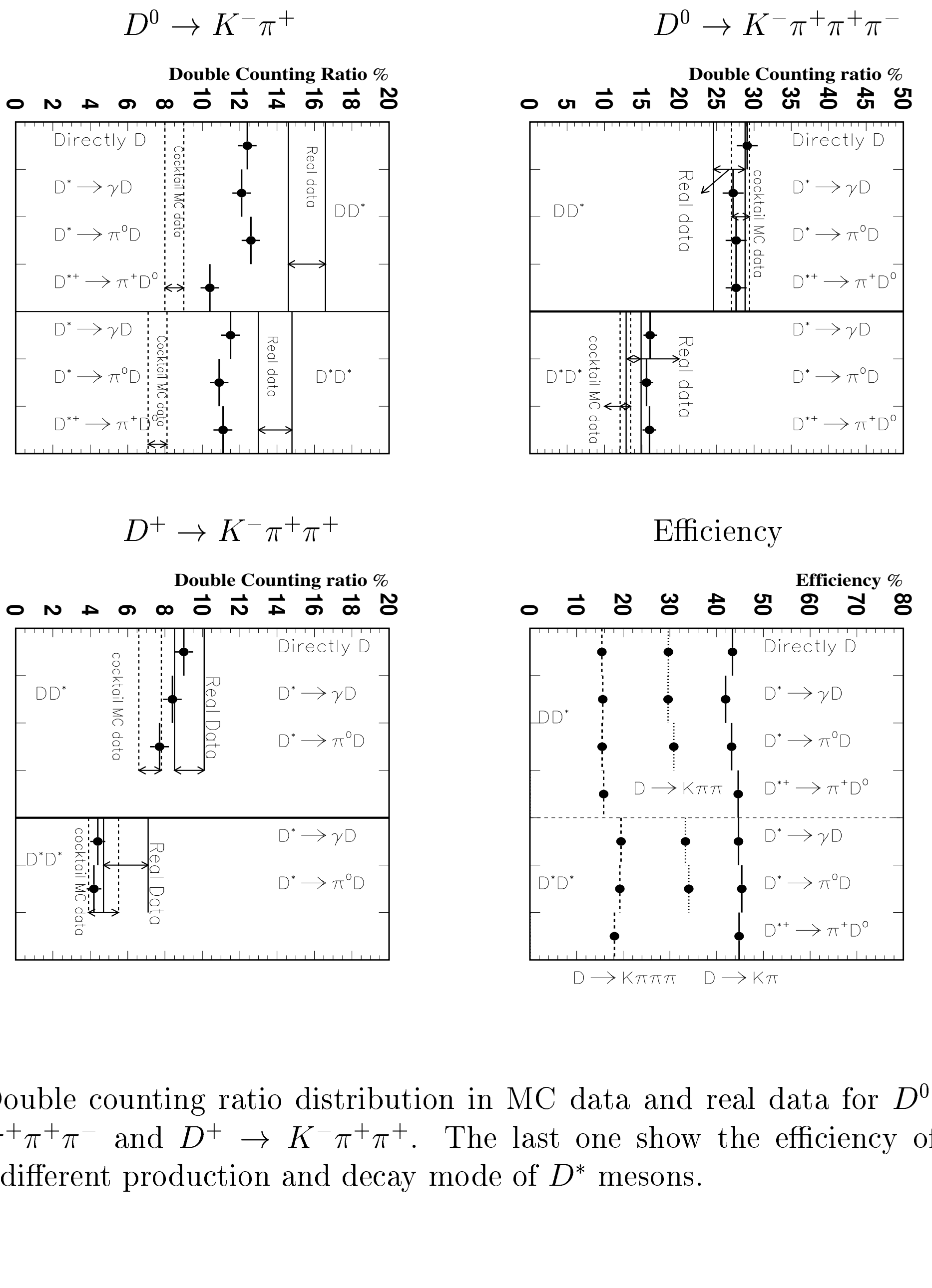

Figure 7: Double counting ratio distribution in MC data and real data for $D^0 \to K^-\pi^+$, $D^0 \to K^-\pi^+\pi^+\pi^-$ and $D^+ \to K^-\pi^+\pi^+$. The last one show the efficiency of single-tag selection in different production and decay mode of D^* mesons.

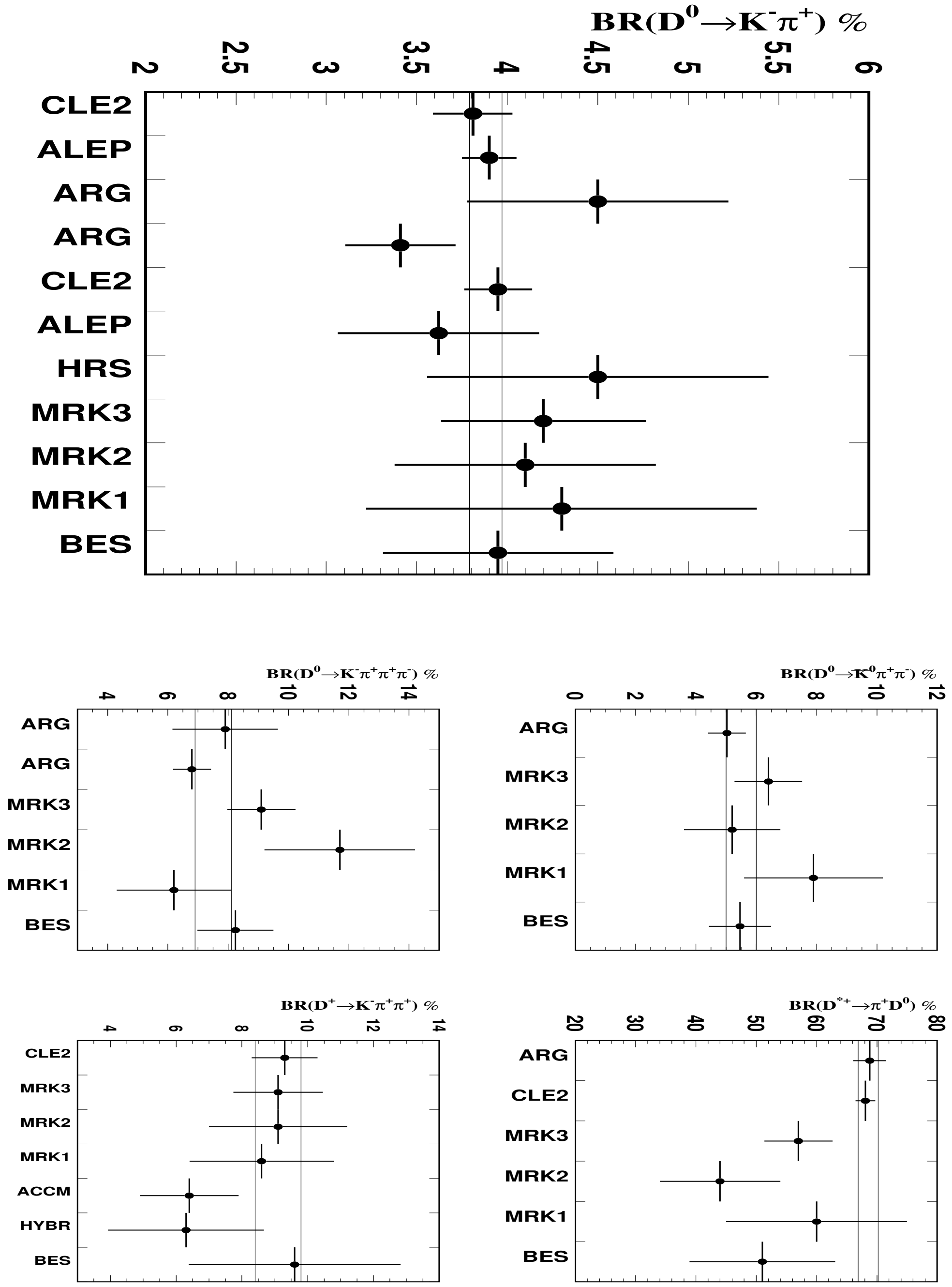

Figure 8: Comparison of $\mathrm{Br}(D^0 \to K^-\pi^+)$, $\mathrm{Br}(D^0 \to K^-\pi^+\pi^+\pi^-)$, $\mathrm{Br}(D^0 \to \overline{K^0}\pi^+\pi^-)$, $\mathrm{Br}(D^+ \to K^-\pi^+\pi^+)$ and $\mathrm{Br}(D^{*+} \to \pi^+ D^0)$ with other experiments.